



Particle motion observed during offshore wind turbine piling operation

Peter Sigray^{a,*}, Markus Linné^b, Mathias H. Andersson^b, Andreas Nöjd^b, Leif K.G. Persson^b, Andrew B. Gill^c, Frank Thomsen^d

^a Royal Institute of Technology, Department of Engineering Mechanics, S-100 44 Stockholm, Sweden

^b Swedish Defence Research Agency, S-164 90 Stockholm, Sweden

^c Centre for Environment, Fisheries and Aquaculture Science (Cefas), Lowestoft, Suffolk NR33 0HT, UK

^d DHI A/S, Agern Allé 5, DK-2970 Hørsholm, Denmark

ARTICLE INFO

Keywords:

Particle motion
Sensor
Piling
Mitigation
Exposure level

ABSTRACT

Measurement of particle motion from an offshore piling event in the North was conducted to determine noise levels. For this purpose, a bespoke sensor was developed that was both autonomous and sensitive up to 2 kHz. The measurement was undertaken both for unmitigated and mitigated piling. Three different types of mitigation techniques were employed. The acceleration zero-to-peak values and the acceleration exposure levels were determined. The results show that inferred mitigation techniques reduce the levels significantly as well as decreases the power content of higher frequencies. These results suggest that mitigation has an effect and will reduce the effect ranges of impact on marine species.

1. Introduction

Particle Motion (PM) is a fundamental component of underwater sound, which is sensed by fish and invertebrates (Nedelec et al., 2016; Popper and Hawkins, 2018). Despite its importance, particle motion has rarely been studied in open water conditions as pointed out by Popper and Hawkins (2018) and never at an offshore piling event. Historically, the focus has been on pressure variations, measured using hydrophones, which are inherently sensitive to pressure despite the fact that in certain situations sound pressure level cannot be used as a proxy for particle motion (Nedelec et al., 2021). The lack of attention on the particle motion component of sound, is reflected in very few appropriately designed autonomous sensors with enough sensitivity, that can be deployed in open sea conditions (Martin et al., 2016; Nedelec et al., 2021). However, greater appreciation of the importance of particle motion in the lives of marine taxa means that sensors are now in demand owing to the growing interest in the input of anthropogenic sound into the marine environment through offshore activities, with the generation of underwater sound predicted to increase even more in the future (Gill et al., 2012; Nedelec et al., 2016). In this study a bespoke particle motion sensor was used to measure for the particle motion from an offshore piling event in the North Sea. The sensing principle is based on a near-neutral buoyancy sphere submerged in the sea with a centrally placed accelerometer that is sensitive to the particle motion induced by

sound waves. The near buoyancy makes sphere impedance of the sphere close to that of the water and if the wavelength of the sound is larger than the diameter of the sphere, the sound wave will not sense the presence of the sphere, which will co-oscillate with the surrounding water and give a direct measurement of the particle motion of the water particles.

One of the main marine sounds producing activities is impulse piling driving, which often is used in constructions of marine infrastructures, such as bridges, wind turbines and harbor facilities. The piling technique generates impulsive noise with high transient sound levels near the piling area at frequencies below 1 kHz (De Jong and Ainslie, 2008; Reinhall and Dahl, 2011; Götsche et al., 2015; Martin and Barclay, 2019). When a hammer strikes the top of the pile an elastic wave is generated, which travels through the structure towards the seabed. As the wave transmits down the pile the energy is reflected at the end cap and the wave continues to radiate sound into the water column and the seabed. The propagating wave in the pile results in an in-water Mach-wave. (Massarsch and Fellenius, 2008; Reinhall and Dahl, 2011; Hazelwood and Macey, 2016). The overall time for securing piles for larger turbines into the sea floor under normal conditions is in the range of hours (Juretzek et al., 2021). This is a time span that not only give rise to a source of high impulsive sound levels of radiated acoustic energy but also to high integrated energy (exposure) over the pile installation time in the piling area. Both entities of which can affect the marine

* Corresponding author at: Royal Institute of Technology, Department of Engineering Mechanics, Teknikringen 8, S-100 44 Stockholm, Sweden.
E-mail address: sigray@kth.se (P. Sigray).

<https://doi.org/10.1016/j.marpolbul.2022.113734>

Received 3 February 2022; Received in revised form 2 May 2022; Accepted 4 May 2022

Available online 26 May 2022

0025-326X/© 2022 The Authors. Published by Elsevier Ltd. This is an open access article under the CC BY license (<http://creativecommons.org/licenses/by/4.0/>).

animals (i.e. the receptors) negatively.

The environmental impact from pile driving on marine animals, in terms of sound pressure has been investigated to some extent for mammals (Madsen et al., 2006; Baily et al., 2010) and fish (Thomsen et al., 2006; Debusschere et al., 2014; Martin and Barclay, 2019). Marine animals with internal air-filled cavities such as mammals and those fish with swim bladders are sensitive to sound pressure. However, sound pressure is not the relevant stimulus for most teleost and elasmobranch fish, and invertebrates and cannot be used for assessing the impact. Instead, the particle motion component of the sound field has to be measured (Fay, 1984; Casper and Mann, 2006; Kaifu et al., 2008; Popper and Fay, 2011). In particular, the acceleration of the water particles is suggested to be the relevant stimuli for these groups of animals (Kalmijn, 1989; Fay and Edds-Walton, 1997). Few studies have been conducted on invertebrates (Solé et al., 2017; Weilgart, 2018).

Despite the well-established knowledge of Particle Motion as a relevant stimulus of sound, there have been few studies on sound source characteristics of a pile driving operation in terms of PM in the water column (MacGillivray and Racca, 2005; Miller et al., 2015; Ceraulo et al., 2016; Jansen et al., 2019) and no with comparison between mitigated and unmitigated piling. Impact studies are also few (Mueller-Blenkle et al., 2010; Magnhagen et al., 2017). This knowledge gap was identified in reviews and guideline papers and relates both to impact studies as well as sound source characteristics (Popper et al., 2014; Hawkins et al., 2015; Nedelec et al., 2016; Nedelec et al., 2021).

A main driver for interest in the impact of underwater sound is to meet Environmental Impact Assessment legislative requirements particularly relating to conservation designated animals (such as marine mammals), which will become even more important as countries worldwide look to meet their policy commitments of net zero carbon emissions, decarbonisation and promotion of green energy (Juretzek et al., 2021). In order to determine environmental impacts, there is a need to quantify the anthropogenic sound source and interpret the results in relation to the impact of the receptor animal of interest. As a first step, this requires suitable instruments for measuring both components of underwater sound. Sound pressure is relatively easily measured. However, technical progress has been slow in terms of developing sensors for particle motion and especially for autonomous use in oceans. Compared to sound pressure, few studies have been conducted where particle motion have been measured (Zeddies et al., 2010; Sigray and Andersson, 2011; Martin et al., 2016).

The paper starts with a short discussion on the design of an autonomous particle motion sensor. Results are presented from particle motion measurements with the bespoke sensor from an in situ field trial of

both unmitigated and mitigated pile driving of a pile for an offshore wind turbine in the North Sea are presented. Finally, methods for analysing the data, results of the sound levels established, and the efficiency of different mitigation techniques are discussed.

2. Method

The particle motion sensor, (henceforth named the “PM-sensor”), is based on the design described in Sigray and Andersson (2011). The sensor system used in this study was specifically designed to fit open ocean conditions such as in the North Sea. It was developed to be autonomous, and the frequency range was extended compared to the earlier design to cover the frequency range of piling. The PM-sensor consisted of two water-proof electronic casings, one with rechargeable lithium batteries and the other contained the data acquisitions system and a tethered sensing sphere (Fig. 1). The dimension of the PM-sensor system was approximately 0.5 m length, 0.5 m width and 0.3 m height and 30–35 kg weight in air. The diameter of the nearly neutrally buoyant sphere was 0.06 m and when deployed floats 0.5 m above the seabed. A PCB Piezotronics, model 356B18, 3-axis accelerometer was mounted inside the sphere. The sensitivity of the accelerometer was $0.1 \text{ V}/(\text{m}/\text{s}^2)$. The sampling frequency was 14,400 Hz and the resolution of the Analog-to-Digital converter was 24 bits. The recorded data were stored on a 32 GB SD-card.

Prior to the field measurement campaign, the sensing sphere was mounted on a shaking table for control of frequency response. The sphere was attached on the table close to a reference accelerometer and the frequency of the table was swept from 1 Hz up to 20 kHz. The results showed that the sensor response was constant in the frequency interval 1 Hz to 2 kHz. To place the sphere in a fix position above the seabed the buoyancy of the sphere was made slightly positive, thereby stretching the tether between the sphere and the casings and keeping the sphere in a fix position relative to the seabed. The difference between sphere and water density introduces a deviation factor of the measured amplitude (McConnell, 2003). A positively buoyant sphere responds with an amplitude that is greater than the acoustic wave, the 6% lighter sphere will give an overestimate of the amplitude of 3% ($0.6 \text{ dB re } 1 \mu\text{m}/\text{s}^2$). The amplitude of the system will however be dictated by the combination of sphere and tether. To determine the correction factor, the PM-sensor was cross-compared with gradiometer-coupled hydrophones in a water filled tank, following the same procedure as was described in Sigray and Andersson (2011) prior to the measurements. The PM-sensor was later cross-compared in free field conditions that confirmed the earlier result obtained in the tank (Linné and Sigray, 2019). The free field calibration

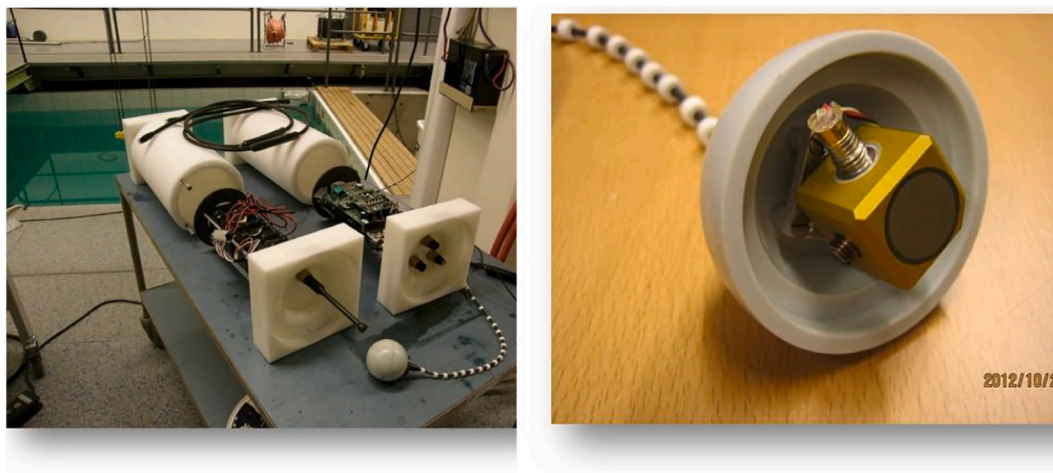


Fig. 1. (a) The two waterproof chambers containing batteries and data acquisition system with sensing sphere shown at the front. (b) Close-up view of one-half of the sensing sphere with the 3-axis accelerometer mounted inside.

was done from 100 Hz to 2 kHz and the 2σ -error was estimated at 100 Hz to be 1.6 dB re $1 \mu\text{m/s}^2$, including the buoyancy, send response, gain, distance, and wetting errors (Linné, 2022). Notably, the 2σ -error includes the deviation from the ideal situation when the sensor is buoyantly neutral. The comparison was done for the three axes combined of the PM-sensor in the frequency range of 40 Hz – 2000 Hz, which covers the relevant frequency range at some hundred meters distance from the piling event as was also found by Juretzek et al. (2021).

2.1. Piling and mitigation techniques

The in situ PM measurements were carried out in 2015 at an offshore wind farm site in the German bight approximately 25 nautical miles from the mainland (Fig. 2). This site contained a large number of operational as well as on-going constructions of wind turbines. In total, the completed windfarm consisted of 42 Siemens SWT turbines with a power rating of 6 MW and a blade diameter of 154 m. During the periods of construction when PM measurements took place, a heavy-lift jack-up vessel was used with a hydraulic hammer (S-3000) to fix the steel piles (65.6 m) into the seabed. Three different types of mitigation techniques were used in different combinations: an air Isolated Steel Barrier (aISB) used in combination with an Internal Bubble Screen (IBS) and a stand-alone Bubble Curtain (BC), deployed outside the aISB (Koschinsky and Lüdemann, 2020). The aISB consists of two metallic cylinder casings concentrically wrapped around the pile all the way from the seabed into air with an air-filled outer space and a bubble filled inner space that decouples the acoustic radiation from the water. This device thus contains two mitigation systems in one. The BC consist of a hose laid on the seabed encircling the whole piling platform. The radius of the bubble curtain was about 100 m. Through the hose is air pumped that forms a cylindrical wall of bubbles stretching from the seabed to the surface thereby acoustically shielding the outer water mass from the acoustic source.

The water depth at the piling site was approximately 30 m and the seabed consisted of sand. Measurement of particle motion generated

from piling was done on two specific piles, denoted as pile A and pile B (Fig. 2). The piling was undertaken on two consecutive nights starting in the evening of 25th April 2015. Active hammer time was 80 min for pile A and 310 min for pile B. Pile A was a standard piling operation using all three mitigation techniques (i.e. full mitigation), whilst pile B was an experimental piling operation where different combinations of mitigation techniques were applied. The hammering rate was approximately 60 strikes per minute during the whole piling operation. The number of strikes to reach set depth was 3323, for pile A and 6308 strikes for pile B. It is notable that the IBS and BC mitigation were turned on and off and the aISB was in place or removed during the piling of pile B.

The PM-sensor was deployed 580 m from pile A before the piling started. The installation of pile A started with a 5-minute soft start and the hammer energy was ramped up from 500 kJ to 1600 kJ. The PM-sensor was retrieved, and recorded data were downloaded. The PM-sensor was re-deployed 880 m from the pile B before piling started (Fig. 2). The piling started with a 5-minute soft start and a ramp up to 500 kJ. Different mitigation techniques were then tested whereafter the energy was raised to 800 kJ. The PM-sensor was finally retrieved after the piling of pile B was finished. Simultaneous measurements of Sound Pressure Level were performed by a private company for the wind farm operator, but data were not accessible to this study due to confidential restrictions.

The sequence of the piling events over two days is shown in Table 1. Pile A was used as a reference site equipped with full mitigation, which included aISB in place, IBS on and BC on, and a nominal hammer energy of 1600 kJ, whilst pile B was used to investigate the efficiency of noise reduction with different mitigation techniques in place as well as to study the influence of hammer energy on the emitted sound field. The aim of the two days of piling was to compare different mitigations techniques applied on pile B, with the full suite of mitigation applied on pile A.

During the measurements the mean wind direction was northerly, and the wind speed varied between 4 and 8 m/s. The wave direction was southward and wave height was between 1 and 2 m with a significant wave height of 1 m. There were occasionally strong currents up to 1.2 knots. The water temperature was approximately 7.5 °C in the whole water column.

3. Data analysis

All data sets were processed in two consecutive steps. In the first, a bandpass filter with cut-off frequencies at 30 and 2000 Hz was applied to remove signal content induced by low frequency wave motion and high frequency sound. The high frequency threshold was dictated by the limitation set by the sensor response (Sigray and Andersson, 2011). All sound levels reported in this study, except spectral levels, refer to broadband levels determined in the frequency interval 30 to 2000 Hz. In the second step, maximum acceleration for each individual hammer strike was localized in time by over-laying a 1-s time window onto the recorded sound, for which the start of piling was set to 0.3 s before the occurrence of the maximum acceleration and 0.8 s after for the end of the window. To estimate the effect of the window length on the derived exposure level, the window time length was decreased from 1 s to 0.9 s, which resulted in a reduction of received energy of 2%. This test showed that most of the energy from a single strike was located inside the 1-s window and thus confirmed the extraction of single strike levels can be used to estimate total exposure levels. Following standard procedures, measurements of background sound were undertaken before and after the piling and sound levels were found to be constant. Hence, to take background levels into account, measured acceleration levels for pile A and pile B were adjusted by subtracting acceleration level corresponding to 1 (re $1 \mu\text{m/s}^2$) dB.

To quantify the received signals, the zero-to-peak acceleration levels and acceleration exposure levels were derived. For each hammer strike, the maximum zero-to-peak level was estimated by using the three axial

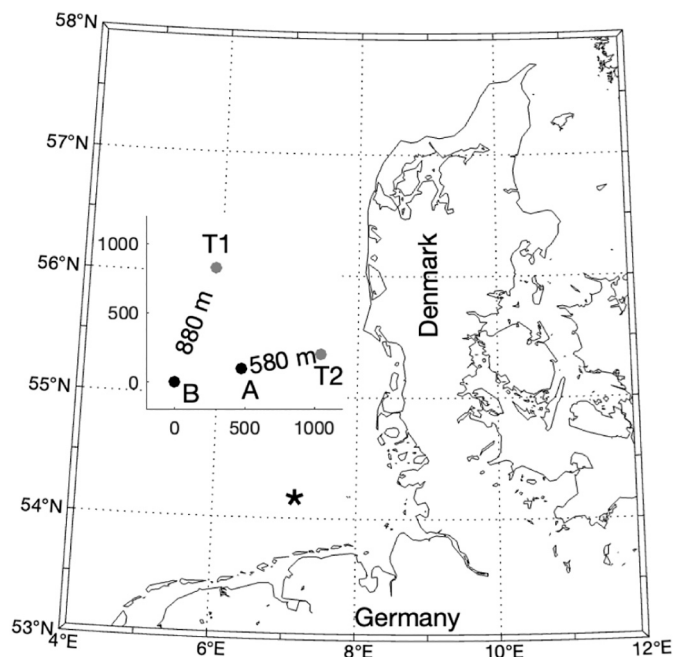


Fig. 2. Map showing the location of the windfarm outside the German coast. Pile A and B are marked. Inset, the location of measurement of Pile A is marked with T1 and for Pile B with T2. The distance between Pile A and the location for the particle motion sensor was 580 m and the distance between Pile B and the sensor was 880 m.

Table 1

Sequence of the applied hammer energy and the mitigation techniques that were used during the measurement of piling noise on pile A and B. The air Isolated Steel Barrier (aISB) was used in combination with the Internal Bubble Screen (IBS). A Bubble Curtain (BC) was used as well. Trial A1 was done with full mitigation and trial B6 was done without any mitigation. The average zero to peak sound particle acceleration level (SAL) and the standard deviation (Std) were estimated for the second half of the piling event where the hammer energy had reached its maximum. The pressure components were used to estimate the average and standard deviations.

| Pile | A | B | | | | | |
|--|-------------|-------------|-------------|-------------|-------------|-------------|-------------|
| Trial | A1 | B1 | B2 | B3 | B4 | B5 | B6 |
| Date | 26/04/2015 | 26/04/2015 | 26/04/2015 | 26/04/2015 | 27/04/2015 | 27/04/2015 | 27/04/2015 |
| Time of piling | 01:24–02:45 | 22:30–22:40 | 22:50–22:55 | 23:05–23:10 | 23:15–23:30 | 01:45–01:55 | 02:00–03:10 |
| Hammer energy (kJ) | 1600 | 500 | 500 | 560 | 800 | 800 | 800 |
| aISB with | In place | In place | In place | In place | In place | removed | removed |
| IBS(on/off) | on | on | off | off | off | removed | removed |
| BC(on/off) | on | on | off | on | off | on | off |
| Average SAL (re 1 $\mu\text{m/s}^2$) dB | 105 | 104 | 119 | 114 | 123 | 116 | 129 |
| Std SAL (re 1 $\mu\text{m/s}^2$) dB | 1.3 | 1.9 | 1.2 | 1.3 | 0.5 | 1.4 | 1.0 |

orthogonal accelerations given by

$$\hat{a} = \sqrt{a_x(t)^2 + a_y(t)^2 + a_z(t)^2} \text{ m/s}^2, \quad (1)$$

where $a_i(t)$ is the acceleration vector component for the x, y z axes relative to the sensor reference plane. The acceleration exposure level for a single strike was estimated by

$$(a_{SS}^E)^2 = \frac{1}{f_s} \sum_{t=t_0}^{t_1} a_x(t)^2 + a_y(t)^2 + a_z(t)^2 \text{ (m/s}^2\text{)}^2, \quad (2)$$

where f_s is the sampling frequency. The acceleration exposure level of multiple events, referred to as the cumulative acceleration exposure level was derived by $a_{CUM}^E = \sum_{n=1}^M a_{SS, n}^E$, where the index n is the strike number summing up to total of M strikes. It is also convenient to express the metrics using the decibel scale. In this study the reference levels $\hat{a}_{ref} = 1 \mu\text{m/s}^2$ and $a_{ref}^E = (1 \mu\text{m/s}^2)^2 \text{ s}$ were used. The zero-to-peak acceleration level was derived by $L_a(\text{re } 1 \mu\text{m/s}^2) = 20 \log(\frac{\hat{a}}{a_{ref}}) \text{ dB}$. Similarly, the single strike and cumulative acceleration exposure levels were derived by $L_{a_{SS}}^E(\text{re } 1 \mu\text{m/s}^2 \text{ s}) = 10 \log(a_{SS}^E/a_{ref}^E) \text{ dB}$, and $L_{a_{CUM}}^E(\text{dB re } (1 \mu\text{m/s}^2)^2 \text{ s}) = 10 \log(\frac{a_{CUM}^E}{a_{ref}^E}) \text{ dB}$.

Using single strike exposure level to estimate the sound exposure level of multiple strikes the following equation can be used

$$SAL_{cum} = SAL_{single} + 10 \log(n), \quad (3)$$

where SAL_{cum} is the cumulative sound acceleration level from n strikes, SAL_{single} is the sound acceleration level from a single strike and n is the number of strikes.

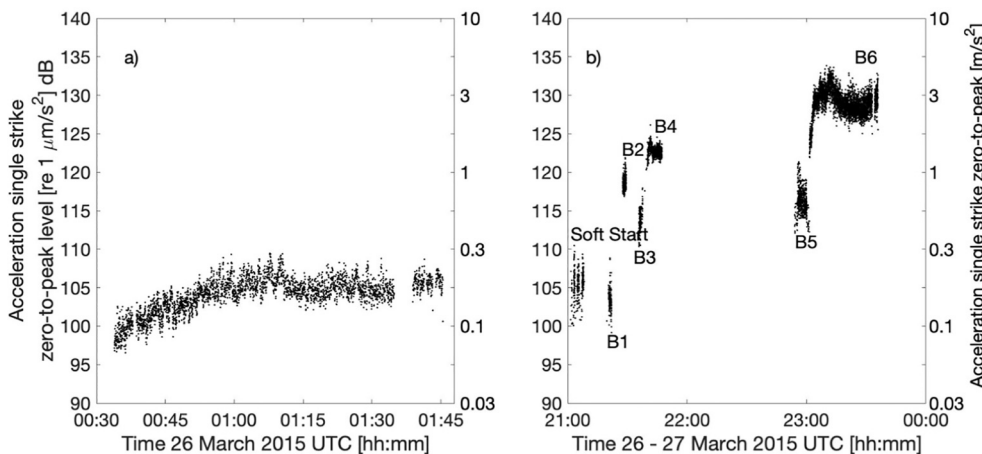


Fig. 3. a) Measured maximum acceleration zero-to-peak values for each strike during the pile A sequence. The levels were obtained with all mitigation techniques in place. The left scale shows the dB levels relative to 1 $\mu\text{m/s}^2$ and the right in SI base units. UTC stands for Coordinated Universal Time. b) Measured maximum acceleration zero-to-peak values for each strike during the pile B sequence. Each trial was separated in time and is marked with corresponding trial number. Refer to Table 1 for details of sequence and mitigation combinations.

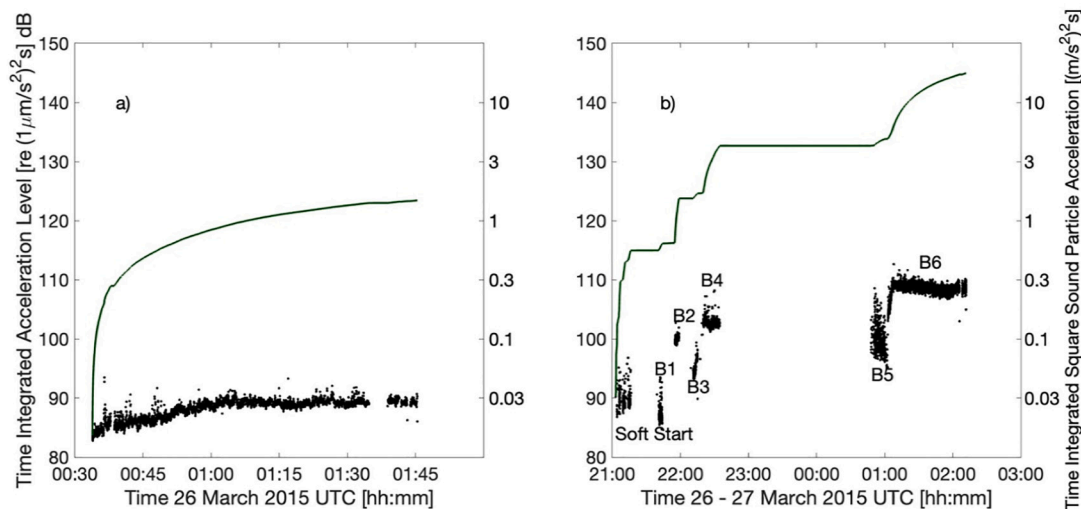


Fig. 4. a) Measured acceleration exposure levels during the pile A mitigated pile driving sequence. The left scale shows the dB levels relative to $1 (\mu\text{m/s}^2)^2\text{s}$ and the right in SI base units. The black line shows the cumulative acceleration exposure levels and the dotted line the acceleration exposure levels for every individual strike. b) Measured acceleration exposure levels during the pile B mitigation test pile driving sequence. Black line shows the cumulative acceleration exposure levels, the dotted black line the acceleration exposure levels for every individual strike. The mitigation tested was separated in time and is marked with corresponding trial number.

and most likely that the difference between fully mitigated (pile A) and unmitigated (pile B6) piling was probably higher than what was observed in this study due to the difference in hammer energy.

Pile A was fully mitigated all the time and thus can be used to study the total acceleration exposure level from the start to the end of a piling event. Based on Eq. (2) the total acceleration exposure level (re $1 (\mu\text{m/s}^2)^2\text{s}$) was 123 dB, which can be compared to a single strike acceleration exposure level (re $1 (\mu\text{m/s}^2)^2\text{s}$) of 89 dB. The analysis was more complex for pile B due to the changes of mitigation techniques, which makes it difficult to compare the results with pile A. Nevertheless, it can be stated that pile B was less mitigated which resulted in a total acceleration exposure level (re $1 (\mu\text{m/s}^2)^2\text{s}$) of 145 dB, which was 22 dB higher compared to trial A1 but notable the first required twice as many strikes. A situation where the same hammer energy is employed is preferred, when comparing an unmitigated with a mitigated piling event. However, the given situation was that the type of mitigation techniques was changed during the piling sequence of pile B. Thus, no full sequence of unmitigated piling was possible to investigate. To circumspect this situation, information from the unmitigated part of trial B6 can be used to estimate a full unmitigated sequence. The estimate has to compensate for scaling of both the hammer energy and the number of strikes as well as to make the assumption that the total number of strikes requested for a hammer energy of 1600 kJ is half the number of strikes for 800 kJ. To correct for the hammer energy (re $1 (\mu\text{m/s}^2)^2\text{s}$) 3 dB is added to a single strike. To rescale the number of strikes is logarithmically added (see Eq. (3)). The total number of strikes for pile B were 6308 and 88% occurred with a hammer energy of 800 kJ. Assuming that all strikes were 800 kJ results in a total exposure level (re $1 (\mu\text{m/s}^2)^2\text{s}$) of 142 dB. Correcting for the hammer energy (i.e. adding +3 dB increases the level (re $1 (\mu\text{m/s}^2)^2\text{s}$) to 145 dB. The last correction is for the number of strikes, which was about twice as many for pile B. Hence, the acceleration exposure level (re $1 (\mu\text{m/s}^2)^2\text{s}$) for pile B is reduced with 3 dB to 142 dB. With all corrections in place, the difference between unmitigated and fully mitigated piling at 1600 kJ adds up to 23 dB.

Finally, a spectral analysis was made to investigate the influence of different mitigation techniques on the spectral content. Power Spectral Densities were estimated for piling event A1, B1, B5 and B6 as well as on background sound. The results are shown in Fig. 5. In general, the unmitigated event (B6) was observed to generate higher levels for all frequencies than the mitigated. It was observed that the mitigation not only

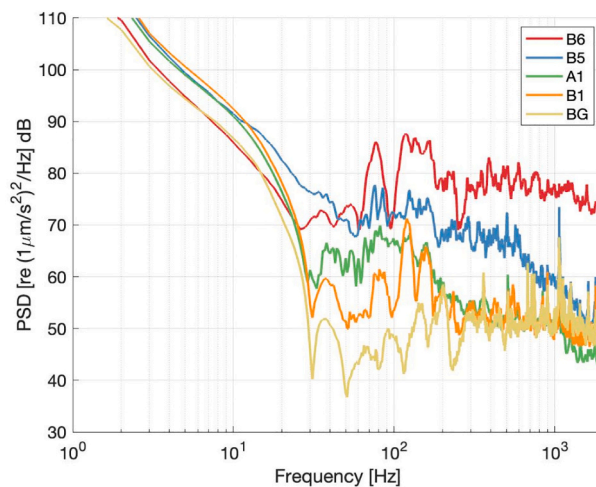


Fig. 5. Power Spectral Density (PSD) levels based on averages of single strikes. The red line shows B6, blue B5, green A1, orange B1 and the yellow line the background when there was no on-going piling activity. Applying mitigation reduces both the sound levels and the high frequency content.

reduced the broadband levels but also had a reducing effect on the high frequency range of the sound. A clear decrease of energy was observed at frequencies higher than 200 Hz for the fully mitigated pile (A1 and B1), for which frequencies higher than 200 Hz the sound pressure levels were comparable with the background noise. With only the BC in place a reduction of frequencies higher than 300 Hz was observed. This response to mitigation was also observed by Juretzek et al. (2021) for sound pressure.

5. Discussion

The study showed how PM can be measured in situ on the seafloor during two pile driving events and how measured levels of PM change depending on mitigation method. This is important when considering the environmental impact on PM sensitive animals such as fish and invertebrates (Popper and Hawkins, 2018; Nedelec et al., 2021).

Even if the sound pressure measurements were not available a coarse

estimate of the sound pressure level can be made using the free field relation between particle motion and sound pressure. The unmitigated trial B6 was used to calculate the sound pressure level by cumulative trapezoidal integration of the PM-data to get the velocity component of the particle motion. By assuming that the free field impedance was valid the zero-to-peak sound pressure level was estimated to be 170 to 175 dB re. $1\mu\text{Pa}$. This value can be compared to the results presented in Juretzek et al. (2021) who obtained 180 dB re. $1\mu\text{Pa}$ at 750 m distance for a hammer energy of 2890 kJ, with mitigation in place. They state that without mitigation the levels were 12 dB higher, thus 192 dB re. $1\mu\text{Pa}$. Compensating the hammer energy of B6 trial level that was 600 kJ to a hammer energy of 2890 kJ adds 7 dB re. $1\mu\text{Pa}$ to the PM deduced sound pressure level, which gives an estimate of 177 to 182 dB re. $1\mu\text{Pa}$. This level is lower than what was regularly observed by Juretzek et al. (2021) but as was pointed out by Nedelec et al. (2021) it can be expected that the PM-levels are attenuated near an interface compared to sound pressure levels, and as a result will underestimate the sound pressure when deduced from particle motion measurements. In this study the sensor sphere was 0.5 m above the seabed, which is near to the seabed. This calculation underlines the importance of measuring PM since it cannot be deducted from sound pressure levels near to an interface such as the seabed. It also shows that the particle motion relation in the water column will change as a function of depth and far from an interface the sound pressure level might be used as a proxy for particle motion.

Spectral estimates of the single strike events at pile A (full mitigation) and pile B (different mitigation combinations) showed that the piling energy at measurement range were found in the frequency interval 30 Hz to 2000 Hz. Gravitational waves dominated the motion below 30 Hz (Fig. 5). The spectral analysis revealed that the peak acceleration was in the interval 100 to 200 Hz with decreasing acceleration levels both at lower and higher frequencies (Fig. 5), which confirms the observation made by Sigray and Andersson (2011). The spectra in Fig. 5 also show that with the BC on, an efficient reduction of high frequency noise was achieved outside the barrier. Most notable was the level of difference obtained by altering between unmitigated and fully mitigation, which clearly demonstrated that the mitigation techniques had a reductive effect on the radiated particle motion level. A full piling sequence was measured from start to set depth (trial A1, pile A). The piling of pile A started with a soft start at a hammer energy of 322 kJ, which was slowly raised to 1600 kJ, clearly visible in the observed acceleration levels shown in Fig. 3. The gap at the end of the piling sequence was due to a planned stop where the inclination of the pile was measured. The set depth of pile A was 30.2 m. The number of strikes needed per 0.25 m penetration was measured by the construction company and varied between 1 and 76, for pile A. It was not possible to pair strikes to the time in Fig. 3 since the installation company only recorded strikes per penetration depth and not time. The 76-strike event could not be attributed to a certain outlier event in Fig. 3. The outliers in Fig. 3 were in the order of 2–3 dB, which indicate that the hardness of the strata at most raised the acceleration level (re $1\mu\text{m/s}^2$) with 2–3 dB.

We were able to measure different combinations of mitigation techniques within the operational schedule dictated by the operator. In total six trials were undertaken, including different piles, hammer energies and mitigation combinations. The trials followed a sequence revealed five important conclusions that can be drawn. First, trial B6 was done with the aISB and IBS removed as well as the BC off, which corresponded to fully unmitigated piling. Trial B5 differed only from B6 in that the BC was on. Consequently, implementation of an external BC reduced the observed acceleration level (re $1\mu\text{m/s}^2$) with 12 dB (broadband). Secondly, with the aISB in place but not activated (trial B4) reduced the observed acceleration level (re $1\mu\text{m/s}^2$) with 5 dB, compared to fully unmitigated piling (trial B6). This implies that the steel barrier itself had a reducing effect even if the IBS was turned off. Thirdly, keeping the aISB in place and turning the IBS off (trial B4) and only activating the BC (trial B3) led to a reduced acceleration level (re $1\mu\text{m/s}^2$) of 9 dB. This result is similar to trial B6 and B5, for which a

reduction of 12 dB was observed. Fourthly, the difference in acceleration level between fully mitigated piling at 1600 kJ and unmitigated at 1600 kJ (based on 800 kJ measurement) was 26 dB. The BC was solely responsible for a reduction of about 12 dB the remaining part, 14 dB, was due to the combination of BC, aISB and IBS. It could be argued that the observed levels were influenced by location and measurement sites for the two piles. However, the distance to pile A was shorter than the distance to pile B and the hammer energy was also higher on pile A. Both these circumstances suggest that actual difference in acceleration levels between pile A and pile B was probably higher than observed. Finally, the introduction of full mitigation (trial A1 and B1) reduced not only the broadband noise levels in but specifically lowered the frequency content above 300 Hz to levels comparable to the background.

The results for time integrated acceleration exposure follow the observed results on acceleration levels, i.e. higher acceleration levels gave rise to higher exposure levels (Fig. 4). The observed acceleration levels were fairly constant during one trial, which suggests that the single strike acceleration exposure levels can be used to derive total acceleration exposure levels (Fig. 4) by using the relation between number of strikes and single strike exposure given in Eq. (3).

The total acceleration exposure level (re $1(\mu\text{m/s}^2)^2\text{s}$) for pile A was observed to be 123 dB. The corrected acceleration exposure level (re $1(\mu\text{m/s}^2)^2\text{s}$) for pile B without any mitigation in place based on single strike exposure was found to be 142 dB.

Whilst this study shows the changes to PM associated with mitigation of pile driving sound, the question of how the mitigation could be effective in the context of affecting PM-sensitive species remains unanswered. It has been shown that elasmobranch fish (the sharks and rays, Casper and Mann, 2006, 2007) have hearing thresholds in terms of particle acceleration about 40 dB higher than teleost fish, such as cod, plaice and salmon (Chapman and Hawkins, 1973; Chapman and Sand, 1974; Hawkins and Johnstone, 1978). There is an issue with comparing thresholds of species with piling sound levels from field conditions. Hearing thresholds for fish are usually obtained using sinusoidal sound in quiet laboratory environment, whilst the sounds associated with piling are transient in character and obtained in noisy environment. Few studies have reported fish reactions to noise in terms of particle motion and even fewer have undertaken dose-response studies. Hawkins et al. (2014) noticed a 50% response level in free swimming sprat (*Sprattus sprattus*) and mackerel (*Scomber scombrus*) when exposing the fish to airgun noise in terms of peak-to-peak particle velocity (re 1 m/s) of -80.4 dB. However, they did not measure velocity directly but calculated it from pressure values using the plane wave equation which makes it difficult to compare their results with results from this study, performed in shallow water, as was pointed out by Nedelec et al. (2016). Mueller-Blenkle et al. (2010) exposed cod (*Gadus morhua*, with a swim bladder, sensitive to PM and pressure) and sole (*Solea solea*, without a swim bladder, sensitive to PM only) to sound play backs from pile driving noise using an underwater speaker system in large net pens and observed significant behaviour reaction when the measured zero-to-peak levels (re $1\mu\text{m/s}^2$) were in the range of 60 dB to 76 dB. A more recent study showed that cod exhibited reduced heart rate (bradycardia), which is an initial flight reaction, in response to sounds from an air gun with zero-to-peak levels (re $1\mu\text{m/s}^2$) of 57–76 dB (Davidson et al., 2019). These values should be compared to zero-to-peak levels (re $1\mu\text{m/s}^2$) of 128 dB obtained in this study and the measured reduction (re $1\mu\text{m/s}^2$) of about 26 dB due to mitigation techniques. At 580 m distance from the piling event the animals will still sense the impulsive noise from fully mitigated pile A. However, the difference between the fully mitigated pile A and background noise levels (re $1\mu\text{m/s}^2$) was only 10 dB, which is a significant reduction compared to the unmitigated pile B. This implies that the zone of potential impact on species is substantially decreased due to the applied mitigation. It should be underlined that despite the applied mitigation techniques, the PM levels are still elevated at some hundred metres distance from the piling event and as a result sensed by many animals, especially immobile organisms.

Behavioural reaction cannot solely be established based on hearing threshold and acceleration levels. However, it can be stated with some confidence that the range where elasmobranch and teleost fish will detect the piling will differ. Further the observed reduction of the acceleration levels (re $1 \mu\text{m/s}^2$) of 26 dB will most likely have an effect on response ranges and might even reduce the levels nearer to hearing thresholds of response for sharks and rays not far from the piling event.

6. Conclusions

In this study a bespoke autonomous PM-sensor was used for observation of particle motion generated from pile driving of an offshore wind turbine foundation in the North Sea. The aim was to investigate the reduction of particle motion levels for different mitigation techniques and hammer energies.

The most striking result was that a reduction of the broadband level (re $1 \mu\text{m/s}^2$) of 26 dB was achieved by employing full mitigation, which consisted of an external BC and an aISB to which an IBS was mounted. The results suggest that the external BC reduced the particle motion (re $1 \mu\text{m/s}^2$) with 12 dB and with the BC, aISB and the IBS in place with (re $1 \mu\text{m/s}^2$) additional 14 dB. The exposure acceleration levels (re $1 (\mu\text{m/s}^2)\text{s}$) for fully mitigated piling was 118 dB and for unmitigated 142 dB. The observed reductions of the particle acceleration levels highlight that mitigation decreased the extent of the radiated PM and therefore will effectively reduce the potential zone of impact to PM-sensitive receptors, with the extent of this zone dependent on the type of mitigation applied.

The spectral analysis of the particle motion for the different mitigation techniques shows that the BC efficiently reduced sound in the range 30 to 1000 Hz with a reduction of high frequency noise starting at 500 Hz. Combined with the aISB and the ISB the range reduced further, to 30 to 300 Hz in line with findings by Juretzek et al. (2021), whose study was based on hydrophones. This reduction of spectral range might have important implications when estimating the impact on animals.

Whilst the results reported here will assist in the consideration of the potential impact of piling noise to PM-sensitive receptors, the apparent mismatch between hearing threshold and impulsive sound underlines the need to derive thresholds using piling-like sound. Further, it is recognized that more studies on particle motion and its impact on marine species should be undertaken and especially in shelf and shallow water areas where a PM cannot be estimated using measurement of sound pressure variation.

Declaration of competing interest

The authors declare that they have no known competing financial interests or personal relationships that could have appeared to influence the work reported in this paper.

Acknowledgement

This study was supported by the MarVEN project (European Commission Directorate for Research and Innovation, RTD-KI-NA-27-738-EN-N2013-2015). We thank Susanna Galloni and Mathijs Soede for their support. We thank Ørsted for the permission and logistical support when undertaking the measurements. We would also like to thank Federica Page (Baker Consultants) for her great help in the field campaign.

References

- Baily, H., Senior, B., Simmons, D., Rusin, J., Picken, G., Thompson, P.M., 2010. Assessing underwater noise levels during pile-driving at an offshore windfarm and its potential effects on marine mammals. *Mar. Pollut. Bull.* 60 (6), 888–897. <https://doi.org/10.1016/j.marpolbul.2010.01.003>.
- Bellmann, M.A., May, A., Wendt, T., Gerlach, S., Remmers, P., Brinkmann, J., 2020. Technical Report Underwater noise during percussive pile driving: Influencing factors on pile-driving noise and technical possibilities to comply with noise mitigation values. ERA Report. Oldenburg, August 2020 (translation of the German

- report version from May 2020). https://www.itap.de/media/experience_report_underwater_era-report.pdf. (Accessed 15 September 2021).
- Casper, B.M., Mann, D.A., 2006. Evoked potential audiograms of the nurse shark (*Ginglymostoma cirratum*) and the yellow stingray (*Urobatis jamaicensis*). *Environ. Biol. Fish* 76, 101–108. <https://doi.org/10.1007/s10641-006-9012-9>.
- Casper, B.M., Mann, D.A., 2007. Dipole hearing measurements in elasmobranch fishes. *J. Exp. Biol.* 210, 75–81. <https://doi.org/10.1242/jeb.02617>.
- Ceraulo, M., Bruintjies, R., Benson, T., Rossington, K., Farina, A., Buscaino, G., 2016. Relationships of sound pressure and particle velocity during pile driving in a flooded dock. *Proc. Mtgs. Acoust.* 27, 040007 <https://doi.org/10.1121/2.0000295>.
- Chapman, C.J., Hawkins, A.D., 1973. A field study of hearing in the cod, *Gadus morhua* L. *J. Comp. Physiol.* 85, 147–167. <https://doi.org/10.1007/BF00696473>.
- Chapman, C.J., Sand, O., 1974. Field studies of hearing in two species of flatfish *Pleuronectes platessa* (L.) and *Limanda limanda* (L.) (Family *Pleuronectidae*). *Comp. Biochem. Physiol. A* 47, 371–385. [https://doi.org/10.1016/0300-9629\(74\)90082-6](https://doi.org/10.1016/0300-9629(74)90082-6).
- Davidson, J.G., Dong, H., Linné, M., Andersson, M.H., Piper, A., Prystay, T., Hvam, E.B., Thorstad, E.B., Whoriskey, F., Cooke, S.J., Sjørusen, A.D., Ronning, L., Netland, T.C., Hawkins, A.D., 2019. Effects of sound exposure from a seismic airgun on heart rate, acceleration and depth use in free-swimming Atlantic cod and saithe. *Conserv. Physiol.* 7 (1), coz020. <https://doi.org/10.1093/conphys/coz020>.
- De Jong, C.A.F., Ainslie, M.A., 2008. Underwater radiated noise due to the piling for the Q7 offshore windfarm park. In: Proceedings of the 9th European Conference on Underwater Acoustics, p. 2987 <http://webitem.com/acoustics2008/acoustics2008/cd1/data/articles/000884.pdf> (accessed 3 February 2022).
- Debusschere, E., De Coensel, B., Bajek, A., Botteldooren, D., Hostens, K., Vanaverbeke, J., Vandendriessche, S., Van Ginderdeuren, S., Vincx, M., Degraer, S., 2014. In situ mortality experiments with juvenile sea bass (*Dicentrarchus labrax*) in relation to impulsive sound levels caused by pile driving of windmill foundations. *PLoS ONE* 9 (10), e109280. <https://doi.org/10.1371/journal.pone.0109280>.
- Fay, R.R., 1984. The goldfish ear codes the axis of acoustic particle motion in three dimensions. *Science* 225, 951–953. <https://doi.org/10.1126/science.6474161>.
- Fay, R.R., Edds-Walton, P.L., 1997. Directional response properties of saccular afferents of the toadfish, *Opsanus tau*. *Hear. Res.* 111, 1–21. [https://doi.org/10.1016/S0378-5955\(97\)00083-X](https://doi.org/10.1016/S0378-5955(97)00083-X).
- Gill, A.B., Bartlett, M., Thomsen, F., 2012. Potential interactions between diadromous fishes of U.K. conservation importance and the electromagnetic fields and subsea noise from marine renewable energy developments. *J. Fish Biol.* 2012 Jul;81(2):664–95. doi: 10.1111/j.1095-8649.2012.03374.x. Erratum in. *Oct J. Fish Biol.* 81 (5), 1791. <https://doi.org/10.1111/j.1095-8649.2012.03374.x>. PMID: 22803729.
- Göttsche, K., Steinhagen, U., Juhl, P., 2015. Numerical evaluation of pile vibration and noise emission during offshore pile driving. *Appl. Acoust.* 99, 51–59. <https://doi.org/10.1016/j.apacoust.2015.05.008>.
- Hawkins, A.D., Johnstone, A.D.F., 1978. The hearing of the Atlantic salmon, *Salmo salar*. *J. Fish Biol.* 13, 655–673. <https://doi.org/10.1111/j.1095-8649.1978.tb03480.x>.
- Hawkins, D.A., Pembroke, A., Popper, A., 2015. Information gaps in understanding the effects of noise on fishes and invertebrates. *Rev. Fish Biol. Fisheries* 25, 39–64. <https://doi.org/10.1007/s11160-014-9369-3>. In this issue.
- Hawkins, A.D., Roberts, L., Cheesman, S., 2014. Responses of free-living coastal pelagic fish to impulsive sounds. *J. Acoust. Soc. Am.* 135, 3101–3116. <https://doi.org/10.1121/1.4870697>.
- Hazelwood, R.A., Macey, P.C., 2016. Intrinsic directional information of ground roll. In: Popper, A.N., Hawkins, A.D. (Eds.), *The Effects of Noise on Aquatic Life II*. Springer, New York, pp. 447–453. https://doi.org/10.1007/978-1-4939-2981-8_53.
- Jansen, Ir.H.W., Brouns, E., Prior, M.K., 2019. Vector sensors and acoustic calibration procedures, TNO 2017 R11589. Den Haag, December 2019. <http://resolver.tudelft.nl/uuid:0ed146dc-4494-4b2e-a434-c75834313968>. (Accessed 15 September 2021).
- Juretzek, C., Schmidt, B., Boethling, M., 2021. Turning scientific knowledge into regulation: effective measures for noise mitigation of pile driving. *J. Mar. Sci. Eng.* 9 (8), 819. <https://doi.org/10.3390/jmse9080819>.
- Kaifu, K., Akamatsu, T., Segawa, S., 2008. Underwater sound detection by cephalopod statocyst. *Fish. Sci.* 74, 781–786. <https://doi.org/10.1111/j.1444-2906.2008.01589.x>.
- Kalmijn, A.J., 1989. Hydrodynamic and acoustic field detection. In: Atema, J., Fay, R., Popper, A., Tavolga, W. (Eds.), *Sensory Biology of Aquatic Animals*. Springer-Verlag, New York, pp. 83–131.
- Koschinsky, S., Lüdemann, K., 2020. Noise mitigation for the construction of increasingly large offshore wind turbines. Report commissioned by the Federal Agency for Nature Conservation, Isle of Vilm, Germany. <https://tethys.pnnl.gov/sites/default/files/publications/Koschinskietal2020.pdf>. (Accessed 2 March 2022).
- Linné, 2022M. Linné (private communication, 2022).
- Linné, M., Sigray, P., 2019. Study of a true free field calibration method of an accelerometer based vector sensor for underwater use. In: UACE2019 - Conference Proceedings, pp. 67–73 https://www.uaconferences.org/component/content/builder/details/22/23/2019_programme-study-of-a-true-free-field-calibration-method-of-an-accelerometer-based-vector-sensor-for-underwater-use (accessed 3 February 2022).
- MacGillivray, A., Racca, R., 2005. In: *Sound Pressure And Particle Velocity Measurements From Marine Pile Driving at Eagle Harbor Maintenance Facility, Bainbridge Island WA*, Prepared by JASCO Research Ltd. for Wa Dept of Transportation, Victoria, British Columbia, Canada, pp. 1–15.
- Madsen, P.T., Wahlberg, M., Tougaard, J., Lucke, K., Tyack, P.L., 2006. Wind turbine underwater noise and marine mammals: implications of current knowledge and data needs. *Mar. Ecol. Prog. Ser.* 309, 279–295. <https://doi.org/10.3354/meps309279>.
- Magnhagen, K., Johansson, K., Sigray, P., 2017. Effects of motorboat noise on foraging behaviour in Eurasian perch and roach: a field experiment. *Mar. Ecol. Prog. Ser.* 564, 115–125. <https://doi.org/10.3354/meps11997>.

- Martin, S.B., Barclay, D.R., 2019. Determining the dependence of marine pile driving sound levels on strike energy, pile penetration, and propagation effects using a linear mixed model based on damped cylindrical spreading. *J. Acoust. Soc. Am.* 146, 109–121. <https://doi.org/10.1121/1.5114797>.
- Martin, B., Zeddies, D.G., Gaudet, B., Richard, J., 2016. Evaluation of three sensor types for particle motion measurement. In: Popper, A.N., Hawkins, A.D. (Eds.), *The Effects of Noise on Aquatic Life II*. Springer, New York, pp. 679–686. https://doi.org/10.1007/978-1-4939-2981-8_82.
- Massarsch, K.R., Fellenius, B.H., 2008. Ground vibrations induced by impact pile driving. In: *Proceedings of the 6th International Conference on Case Histories in Geotechnical Engineering*, Arlington, VA, 11–16 August 2008 <http://webitem.com/acoustics2008/acoustics2008/cd1/data/articles/000884.pdf> (accessed 3 February 2022).
- McConnell, J., 2003. Analysis of a compliantly suspended acoustic sensor. *J. Acoust. Soc. Am.* 113, 1395–1405. <https://doi.org/10.1121/1.1542646>.
- Miller, J.H., Potty, G.R., Kim, H.-K., 2015. Pile-driving pressure and particle velocity at the seabed: quantifying effects on crustaceans and groundfish. In: Popper, A.N., Hawkins, A. (Eds.), *The Effects of Noise on Aquatic Life II, Advances in Experimental Medicine And Biology*, 875, pp. 719–728. https://doi.org/10.1007/978-1-4939-2981-8_87.
- Mueller-Blenkle, C., Gill, A.B., McGregor, P.K., Metcalfe, J., Bendall, V., Wood, D., Andersson, M.H., Sigray, P., Thomsen, F., 2010. Behavioural reactions of cod and sole to playback of pile driving sound. *J. Acoust. Soc. Am.* 128, 2331. <https://doi.org/10.1121/1.3508242>.
- Nedelec, S.L., Campbell, J., Radford, A.N., Simpson, S.D., Merchant, N., 2016. Particle motion: the missing link in underwater acoustic ecology. *Methods Ecol. Evol.* 7, 1–7. <https://doi.org/10.1111/2041-210X.12544>.
- Nedelec, S.L., Ainslie, M.A., Andersson, M.H., Cheong, S.H., Halvorsen, M.B., Linné, M., Martin, B., Nöjd, A., Robinson, S., Simpson, S.D., Wang, L., Ward, J., 2021. *Best Practice Guide for Underwater Particle Motion Measurement for Biological Applications*. Technical report by the University of Exeter for the IOGP Marine Sound and Life Joint Industry Programme.
- Popper, A.N., Fay, R.R., 2011. Rethinking sound detection by fishes. *Hearing Res.* 273 (1–2), 25–36. <https://doi.org/10.1016/j.heares.2009.12.023>.
- Popper, A.N., Hawkins, A.D., 2018. The importance of particle motion to fishes and invertebrates. *J. Acoust. Soc. Am.* 143, 470–488. <https://doi.org/10.1121/1.5021594>.
- Popper, A.N., Hawkins, A.D., Fay, R.R., Mann, D.A., Bartol, S., Carlson, T.J., Coombs, S., Ellison, W.T., Gentry, R.L., Halvorsen, M.B., Løkkeborg, S., Rogers, P.H., Southall, B. L., Zeddies, D.G., Tavolga, W.N., 2014. Sound exposure guidelines for fishes and sea turtles. In: *ASA S3/SC1.4 TR-2014 Sound Exposure Guidelines for Fishes And Sea Turtles: A Technical Report Prepared by ANSI-Accredited Standards Committee S3/SC1 And Registered With ANSI*. SpringerBriefs in Oceanography. Springer, Cham. https://doi.org/10.1007/978-3-319-06659-2_7.
- Reinhall, P.G., Dahl, P.H., 2011. Underwater Mach wave radiation from impact pile driving: theory and observation. *J. Acoust. Soc. Am.* 130, 1209–1216. <https://doi.org/10.1121/1.3614540>.
- Sigray, P., Andersson, M.H., 2011. Particle motion measured at an operational wind turbine in relation to hearing sensitivity in fish. *J. Acoust. Soc. Am.* 130, 200–207. <https://doi.org/10.1121/1.3596464>.
- Solé, M., Sigray, P., Lenoir, M., Van Der Schaar, M., Lalander, E., André, M., 2017. Offshore exposure experiments on cuttlefish indicate received sound pressure and particle motion levels associated with acoustic trauma. *Sci. Rep.* 7, 45899. <https://doi.org/10.1038/srep45899>.
- Thomsen, F., Ludemann, K., Kafemann, R., Piper, W., 2006. Effects of offshore wind farm noise on marine mammals and fish, biola, Hamburg, Germany on behalf of COWRIE Ltd. https://tethys.pnnl.gov/sites/default/files/publications/Effects_of_offshore_wind_farm_noise_on_marine-mammals_and_fish-1-.pdf. (Accessed 2 March 2022).
- Weilgart, 2018. The impact of ocean noise pollution on fish and invertebrates. Report for OceanCare, Switzerland, 23 pp. https://www.oceancare.org/wp-content/uploads/2017/10/OceanNoise_FishInvertebrates_May2018.pdf. (Accessed 2 March 2022).
- Zeddies, D.G., Fay, R.R., Alderks, P.W., Shaub, K.S., Sisneros, J.A., 2010. Sound source localization by the plainfin midshipman fish, *Porichthys notatus*. *J. Acoust. Soc. Am.* 127, 3104–3113. <https://doi.org/10.1121/1.3365261>.